The Nature of the Adsorption of Nucleobases on the Gold [111] Surface

Stefano Piana* and Ante Bilic

Nanochemistry Research Institute, Curtin University of Technology, GPO Box U1987, 6845 Perth, Western Australia

Received: July 13, 2006; In Final Form: September 11, 2006

Biochip technology is based on the immobilization of biological macromolecules on the surface of electronic devices. The biochemical properties of the immobilized molecules can be influenced to a large extent by the interaction with the inorganic surface. The interaction of DNA with the surface of gold, a metal commonly used in biochip technologies, is sequence dependent as the four nucleobases, adenine, thymine, cytosine, and guanine, interact to a different extent with the gold surface. The nature of nucleobase adsorption on the gold [111] surface has been investigated by performing density functional theory and post-Hartree−Fock calculations. It turns out that the interaction is dominated by dispersion forces and an appreciable degree of chemisorption is observed for adenine only. A set of Lennard-Jones parameters that describe the interaction was derived from the post-Hartree−Fock calculations. Classical molecular dynamics simulations of nucleobase monolayers based on these parameters are in remarkable agreement with the experiment and show that the interaction of the nucleobases with the gold surface is strongly modulated by base−base interations and reaches a maximum when a full monolayer is formed.

Introduction

With the development of DNA microarray techniques there has been particular interest in understanding the physics of the interaction of the DNA molecules with the surface of gold-coated electrodes. The strength of the interaction between DNA and the gold surface appears to be sequence-dependent[1] and several Atomic Force Microscopy (AFM)[2−4] and temperature desorption[5,6] studies have been devoted to investigating the structural properties and the energetic of the adsorption of nucleobases on the gold surface. It has been found that, in solution, adenine (A), cytosine (C), and thymine (T) have the tendency to self-assemble in ordered monolayers, while guanine (G) does not form such ordered structures.[2,3] The relative heat of desorption ΔH_{des} of the four DNA nucleobases in a vacuum is guanine > adenine ≈ cytosine > thymine.[5,6] The interaction of the nucleobases with the gold surface is expected to be dominated by dispersion interactions. However, from a simple heavy atoms count, the relative adsorption energy expected for a pure van der Waals interaction between the nucleobases and the gold surface should be guanine > adenine > thymine > cytosine. This observation suggests that other factors may play a role in determining the interaction energy with the gold surface. To shed light on this issue, the structural and electronic properties of the adsorption of the four nucleobases on the gold [111] surface have been determined with DFT calculations. Post-Hartree−Fock calculations have been performed on model systems to derive a set of Lennard-Jones parameters to describe the interaction. On the basis of these parameters, classical molecular dynamics simulations have been performed at different levels of coverage. The calculations show that the interaction with the gold surface is dominated by dispersion interactions. However, at full monolayer coverage, the interaction with the surface accounts only for a fraction of the overall adsorption energy and a significant amount of stabilization comes from the interaction between the nucleobases themselves.

Methods

DFT Calculations. Gradient corrected DFT calculations of nucleobases in contact with the gold surface were performed with the PWSCF[7] program and the PW91[8] exchange-correlation functional. A plane-wave basis set with a cutoff of 25 Ry and Vanderbilt ultrasoft pseudopotentials[9] were used. Test calculations performed with the same computational setup and the PBE[10] exchange correlation functional or with the PW91 exchange-correlation functional and a cutoff of 40 Ry gave similar results in terms of structures and energies. Another set of control calculations was performed with the PBE and PW91 exchange-correlation functionals, a plane wave basis set cutoff of 50 Ry, and Troullier-Martins norm conserving pseudopotentials.[11] The CPMD[12] program was used for this set of calculations. It turns out that the position and orientation of the nucleobases on the gold surface is not affected by the choice of the pseudopotential. However, with the Troullier-Martins pseudopotentials a positive binding energy of 30, 13, 31, and 16 kJ mol^{-1} is obtained for adenine, cytosine, thymine, and guanine, respectively. Finally, the BLYP[13,14] exchange-correlation functional was also tested. It is found that it gives poor results for the structure of bulk gold (the bulk Au−Au distance is 0.04 nm larger than the experimental value), in agreement with previous calculations.[15] For this reason, results obtained with this functional are not discussed in this work.

Geometry optimizations were performed with the conjugate gradient method and a convergence criterion of 10 kJ mol^{-1} nm^{-1} on the largest component of the force. Each system investigated was composed of a nucleobase and 4 layers of 36 gold atoms each. The gold slabs were separated by a 1.2 nm vacuum layer in the direction orthogonal to the surface. The starting position of the nucleobases was 0.5 nm away from the gold surface. A total of 1500 steps of simulated annealing from 100 to 10 K were performed before starting the first geometry optimization (Troullier-Martins pseudopotentials and the PBE

10.1021/jp064438i CCC: $33.50
Published on Web 10/24/2006

exchange-correlation functional). All subsequent optimizations were restarted from the final structure of the first calculation.

Post-Hartree−Fock Calculations. Post-Hartree−Fock calculations were performed with the Gaussian03 program,[16] the Møller−Plesset second-order perturbation theory (MP2),[17] and the Stuttgart/Dresden (SDD) basis set.[18] Calculations were performed for systems composed of small molecules in contact with a planar 4 atom gold cluster. The molecules investigated were hydrogen, methane, ethane, ethylene, amino ethene, formaldehyde, benzene, and imidazole. The structure of the isolated gold cluster was first optimized and kept fixed in all subsequent calculations. The distance between one atom of the molecule and the gold cluster was varied from ∼0.2 to ∼0.6 nm in steps of 0.01 nm. For each step the geometry of the system was relaxed with a convergence criteria of 20 kJ mol^{-1} nm^{-1} on the largest component of the force and 3×10^{-4} nm on the largest displacement. A basis set superimposition error (BSSE) correction[19] was applied through all the calculations. The energy versus distance profiles obtained were used as a reference to perform a least-squares fit of a set of Lennard-Jones parameters (Table 1).

Classical MD Simulations. Classical MD simulations of nucleobases in contact with the gold surface at different coverage were performed with the Gromacs program.[20] The gold surface was modeled as a 3.5534×3.5534 nm^2 2D periodic system with a depth of four layers, for a total of 576 gold atoms. The system was made 3D periodic with a distance of 3.5 nm between the surface images. The dimensions of the final rhombohedral cell were the following: $a = b = 3.5534$ nm, $c = 3.5$ nm, $\alpha = \beta = 90°$, $\gamma = 60°$. The empty space was filled with a variable number of nucleobases ranging from 1 to 80. The simulations were performed with the GROMOS force field[21] modified to include the gold−nucleobase interaction parameters developed in this work (Table 1). The time step for the simulations was 2 fs. A cutoff of 0.8 nm was used for the nonbonded interactions, and long-range electrostatic interactions were treated with the Particle Mesh Ewald method.[22] NVT calculations were performed by coupling the system to a Berendsen thermostat[23] with a relaxation time of 2.0 ps. After 1000 steps of geometry optimization, each system was heated to 600 K for 40 ps and then gradually cooled to 240 K in 400 ps of MD simulation. The final structure of the simulation was geometry optimized and used to calculate binding energies. During the classical simulations the gold atoms were restrained to their starting position with a harmonic force constant of 10 000 kJ mol^{-1} nm^{-1}. As a first test for the parameters developed from the post-Hartree−Fock calculations, the adsorption energies of monolayers of methane, ethylene, benzene, and pyridine were calculated. These calculations involved the simulated annealing of a gold slab and 50 molecules of adsorbate, followed by 1000 steps of geometry optimization.

Results and Discussion

DFT Calculations. The structural and electronic properties of the four nucleobases on the gold surface were investigated by performing DFT calculations with Vanderbilt ultrasoft pseudopotentials and the PW91 exchange-correlation functional. Figure 1 shows the geometry-optimized position of the four nucleobases on the [111] surface of gold. In all the calculations, performed at low coverage in a vacuum, the preferred orientation for the nucleobases is parallel to the surface. This is at variance with IR measurements at high coverage that indicate that all nucleobases are tilted to some extent with respect to the surface.[6]

Consistently with previous studies on related systems,[15] a small relaxation of the outer layer of the gold surface is observed

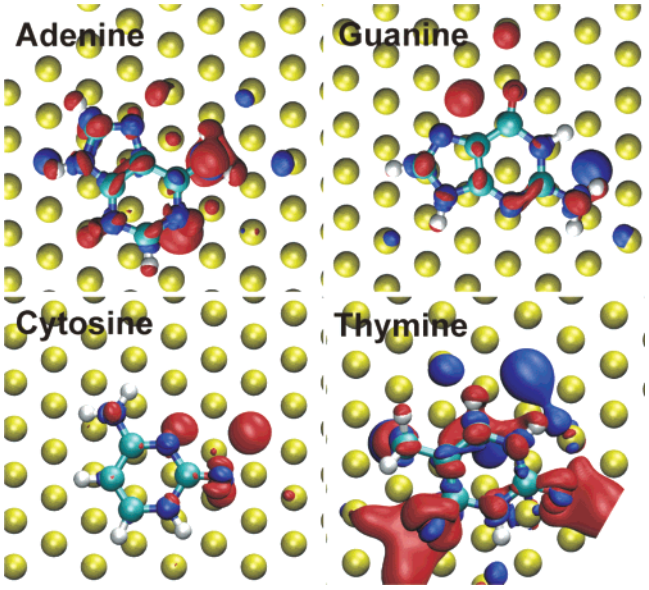

Figure 1. Differential electronic density of the four DNA nucleobases on the gold [111] surface. The polarization induced by the interaction is shown as the difference between the total electron density and the electron density of the isolated systems. Regions of increased electron density are indicated in blue (+1.5 e nm^{-3}), while regions of decreased electron density are indicated in red (−1.5 e nm^{-3}).

in the isolated [111] surface calculations. Upon adsorption of the nucleobases, the surface structure remains essentially unchanged, the largest displacement of a surface gold atom being <0.005 nm. The binding energy calculated within the DFT approach is small, ranging from −5 kJ mol^{-1} for thymine to −13 kJ mol^{-1} for adenine and to −17 kJ mol^{-1} for cytosine and guanine. Experimental adsorption energies for the monolayer range between −105 and −150 kJ mol^{-1}.[5,6] The same results were obtained with the PBE exchange-correlation functional, indicating that the calculations are robust with respect to the choice of functional. Previous studies have shown that this interaction energy is likely to be an artifact of the PW91 and PBE functionals that have the tendency to overestimate the binding energy of weakly overlapping electronic densities.[24,25]

Substantial charge polarization of the gold surface is observed, especially for thymine; however, this polarization appears to contribute little to the binding, in line with previous studies of small molecule adsorption on the gold surface.[25] A comparison of the density of states of the isolated and adsorbed nucleobases reveals only minor perturbation in the electronic structure with the largest variations in the relative orbital energies being less than 10 kJ mol^{-1}. Accordingly, the largest difference in bond length between an isolated nucleobase and a nucleobase adsorbed on the gold surface is 0.001 nm. We conclude that the interactions between the gold surfaces and the nucleobases should be described as a physisorption. Indeed, at low coverage the nucleobases adopt the flat conformation as it allows maximizing the overlap of electronic densities that is responsible for the spurious PW91 attractive interaction. The only exception to this trend is adenine, where a weak chemical bond between the amino group and a gold atom is formed. This interaction leads to a build-up of electronic density between the two atoms and loss of planarity of the amino group (Figure 2). Furthermore, to maximize this N−Au interaction, the nucleobase is tilted at an angle of 10° with respect to the gold surface.

These observations are consistent with IR measurements that show a change of conformation of the $-NH_2$ group when adenine is adsorbed on a gold surface.[5,6] However, the perturba-

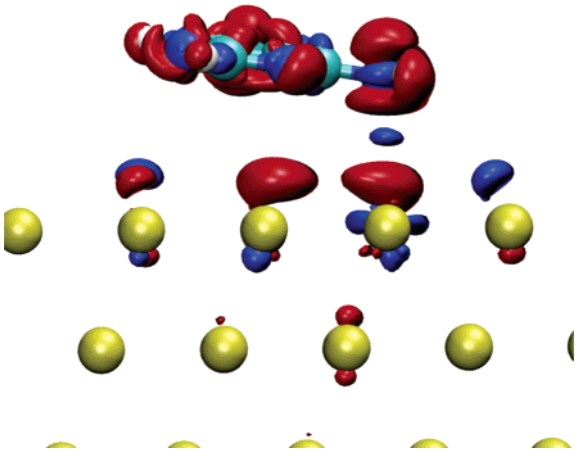

Figure 2. Electronic structure of adenine on the gold [111] surface. Difference between the electronic densities of isolated adenine and gold and the electronic density of the adenine−gold system. Blue areas indicate an increase of electronic density (+1.5 e nm^{-3}) while red areas indicate a decrease in electronic density (−1.5 e nm^{-3}).

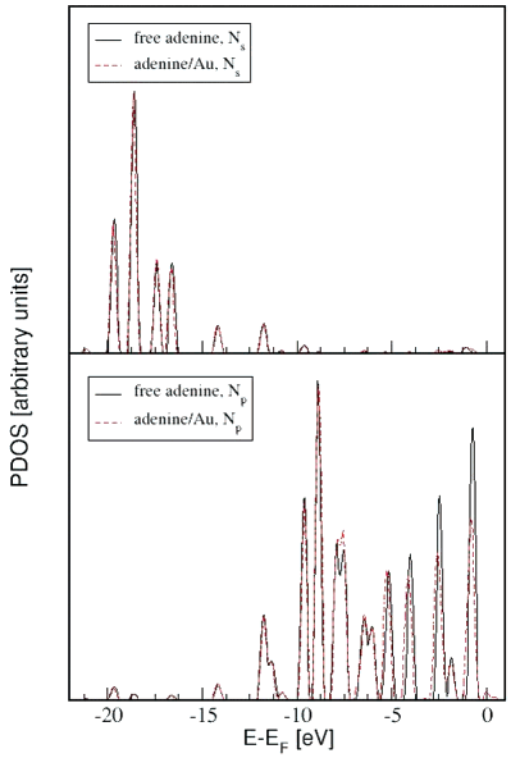

Figure 3. Projected density of states (PDOS) on the s and p orbitals of the nitrogen atom of adenine involved in coordination to the gold surface. The PDOS has been calculated for the isolated nucleobase (black) and for the nucleobase adsorbed on the gold surface (red).

tion to the electronic structure due to this binding is still small, as shown by the projected density of states (PDOS) calculated for the s and p orbitals of the nitrogen atom involved in coordination to the gold surface (Figure 3). Furthermore, the binding of adenine is not stronger than those of the other nucleobases, indicating that the energy involved in this interaction is less than 10 kJ mol^{-1}, much lower than that of a typical chemical bond. In summary, the DFT calculations indicate that for cytosine, thymine, and guanine the extent of chemisorption is negligible, For adenine a very weak chemisorption is observed. Dispersion interactions, which are not present in the DFT approach, are therefore expected to dominate the interaction. The situation may be different for adsorption on a rough or defective surface. Indeed, in recent DFT calculations

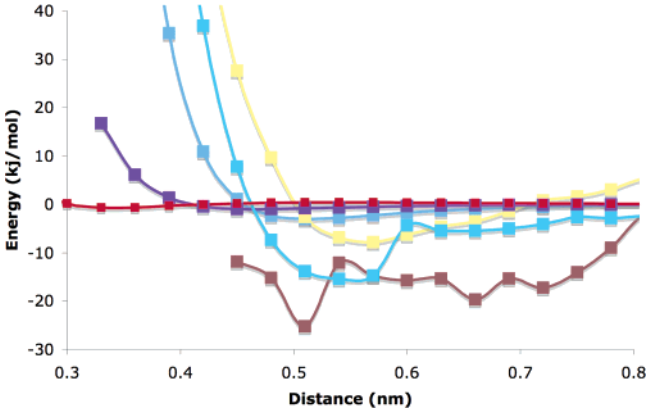

Figure 4. BSSE corrected MP2 energies (kJ mol^{-1}) plotted as a function of distance (nm). Binding energies calculated for hydrogen (red), formaldehyde (purple), benzene (yellow), ethylene (blue), aminoethene (cyan), and imidazole (brown) interacting with the face of a 4 atom gold cluster as a function of the distance of one atom of the molecule from the center of the gold cluster.

performed on small gold clusters, significant chemisorption is observed.[26] Recent studies on the adsorption of phenantroline on the gold surface indicate that this molecule is able to induce reconstruction of the gold surface with creation of adatom sites where chemisorption is observed (P. F. Cafe, and J. R. Reimers, personal communication). We suggest that a similar mechanism may be responsible for the high energy peak observed for adenine in thermal desorption experiments.[6]

MP2 Calculations. Ideally, to study the interaction between the nucleobases and the gold surfaces it should be necessary to perform post-Hartree−Fock calculations of the whole surface−nucleobase system. Unfortunately, this calculation is extremely demanding due to the large number of electrons involved and the large number of degrees of freedom of the system. A different approach was therefore followed in this work. Binding energies between small molecules and the face of a planar 4 atom gold cluster were calculated at the MP2 level. Dispersion interactions between the molecules and the gold cluster were then decomposed as a sum of atomic contributions. In this way, the results of these small molecule calculations were used as a reference to derive Lennard-Jones parameters to describe the nucleobase−surface interaction. The following molecules were considered: hydrogen, methane, ethane, ethylene, amino ethene, formaldehyde, benzene, and imidazole. These molecules contain analogues of all the functional groups that are found in nucleobases. The distance between one of the atoms of the molecule and the center of the gold cluster was constrained to values ranging between 0.3 and 0.8 nm; the system was allowed to relax and BSSE corrected binding energies were calculated (Figure 4). Lennard-Jones parameters were derived by defining atom types for each functional group and simultaneously least-squares fitting all the energy versus distance plots. The resulting parameters are reported in Table 1.

The parameters obtained were tested by performing classical MD simulations of monolayers of methane, ethylene, benzene, and pyridine adsorbed on the gold [111] surface. The calculated adsorption energies for methane, ethylene, benzene, and pyridine (−11.1, −23.4, −57.7, and −72.7 kJ mol^{-1}, respectively) are in good agreement with the values reported in the literature (−14,[27] −24,[27] −57,[27] and ∼−80[28] kJ mol^{-1}, respectively) indicating that, for these simple molecules, the parameters are able to capture the essential features of the adsorption process.

Classical MD Simulations. Classical MD simulations were performed to assess the usefulness of the Lennard-Jones

TABLE 1: Lennard-Jones Parameters for Interaction with Gold Obtained from the Least-Squares Fit to the MP2 Energies[a]

atom type	C_6 (kJ mol^{-1} nm^{-6})	C_{12} (kJ mol^{-1} nm^{-12})
O	7.4675861×10^{-3}	1.3755061×10^{-5}
N (>NH, $-NH_2$, $-NH_3^+$)	8.4639005×10^{-3}	4.7240471×10^{-7}
N_{Ar} (aromatic nitrogen)	4.4433111×10^{-3}	9.5102098×10^{-7}
N_H (aromatic, protonated)	2.8654709×10^{-2}	5.8777336×10^{-5}
C (sp^3, united atom)	9.2101200×10^{-3}	6.2622217×10^{-5}
C (sp^3, all atom)	5.3171953×10^{-3}	1.6812934×10^{-5}
C (sp^2)	3.5163863×10^{-3}	1.3948824×10^{-6}
H	1.2886163×10^{-3}	2.4979847×10^{-6}

[a] Lennard-Jones energies are calculated as: $E_{LJ} = C_6/r^6 + C_{12}/r^{12}$.

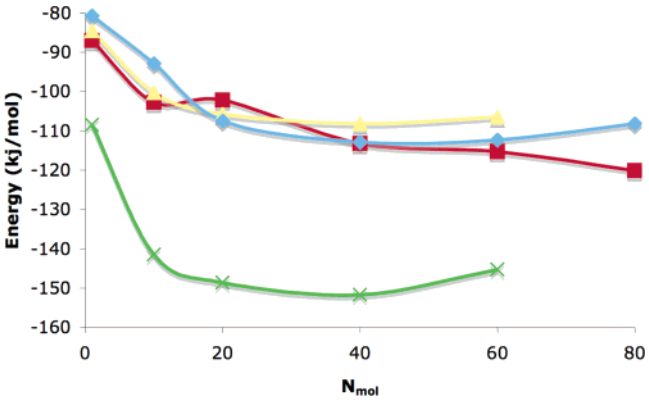

Figure 5. Adsorption energies (kJ mol^{-1}) plotted as a function of the number of molecules (N_{mol}) present in the simulation. Values for adenine (red), cytosine (blue), thymine (yellow), and guanine (green) are reported. Monolayer coverage is achieved for $N_{mol} \approx 40$ for cytosine, thymine, and guanine. A larger number of molecules (about 80) are required for adenine due to its tendency to form stacked arrays.

parameters derived in the previous section to describe the interaction of nucleobases with the gold surface. To this end, the binding energy of nucleobases with the gold surface was calculated at different levels of coverage and compared with the experimental values. The simulations show that, in all cases, the surface binding is cooperative and increases as the surface coverage increases to reach a maximum at the monolayer (Figure 5). The calculated adsorption enthalpies (-120, -113, -108, and -150 kJ mol^{-1} for A, C, T, and G, respectively) are in remarkable agreement with the experimental results ($-124-131$, $-122-130$, $-104-111$, and $-127-150$ kJ mol^{-1} for A, C, T, and G, respectively),[5,6] with the exception of the value for cytosine, which appears to be slightly underestimated by the classical calculations. These results indicate that the simple Lennard-Jones parametrization derived from the MP2 calculations is already providing a reasonable representation of the interaction even if chemisorption and polarization of the gold surface is not explicitly included in this model. Interestingly, isolated bases are found to lie flat on the gold surface to maximize the dispersion interaction. However, as the coverage increases, base−base interactions become competitive with base−surface interactions.

In the case of pyrimidines the base−surface interaction is still dominant and, in the monolayer, the bases are still almost parallel to the surface (Figure 6b,c). In our calculations, cytosine forms a monolayer stabilized by a network of hydrogen bonds where the rings form an approximately hexagonal lattice. This arrangement is similar to the monolayer structure observed in water.[4] The structure of the thymine monolayer appears to be slightly less ordered; this could be consistent with the lower tendency of thymine to form ordered structures.[4] For adenine, a change from parallel to orthogonal orientation is observed

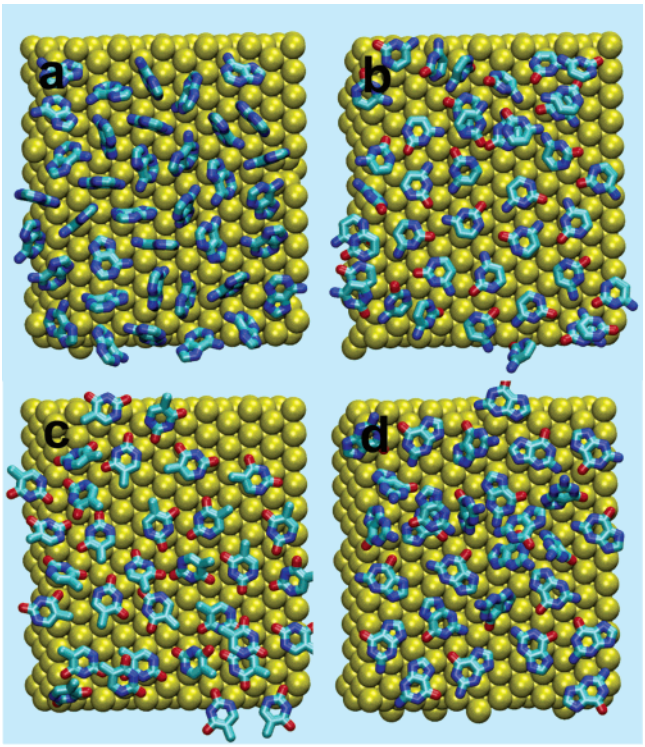

Figure 6. Structure of the monolayers of adenine (a, upper panel left), cytosine (b, upper panel right), thymine (c, lower panel left), and guanine (d, lower panel right) on the [111] surface of gold as obtained from the classical MD simulations with 60 nucleobase molecules. Hydrogen atoms are not shown for the sake of clarity.

(Figure 6a), together with the formation of small regions of ordered arrays of nucleobases. This is consistent with the experimental observation that in solution adenine has the strongest tendency to form ordered monolayers.[2−4] The formation of a highly ordered monolayer is not observed in any simulation, but this is not surprising due to the very slow kinetic of monolayer formation compared to the short time investigated here. Furthermore, the unit cell used in the classical calculations may not be commensurate with the monolayer unit cell, thus frustrating the formation of highly ordered patterns.

An obvious limitation of this approach is that it does not take into account chemisorption and surface reconstruction. These phenomena may be important to correctly describe the complicated adsorption pattern of adenine.[6] However, the classical simulations presented here already provide results that are consistent with the experimental observation both from a structural and from an energetic point of view with a modest computational effort.

Conclusions

In summary, negligible chemisorption is observed in density functional theory calculations of guanine, thymine, and cytosine adsorbed on the gold [111] surface. Very weak chemisorption is observed for adenine only. Parameters to describe the interaction with a Lennard-Jones functional form have been derived from small model MP2 calculations. The adsorption energies calculated with these parameters are in very good agreement with the experimental results. The classical simulations indicate that the adsorption is cooperative and that for adenine, cytosine, and guanine base−base interactions are competitive with base−surface interactions. The parameters developed in this work are expected to be useful in the study of the interaction between DNA with the gold surface, which plays an important role in the field of biochip technology.

Acknowledgment. S.P. thanks Paolo Carloni and Giacinto Scoles for several useful discussions. This research has been supported by the Australian Research Council through Discovery Project DP0558938 and by the government of Western Australia through the Premier research fellowship scheme. Supercomputing time has been provided by CINECA through an INFM grant and by APAC through the Merit Allocation Scheme.

References and Notes

(1) Storhoff, J. J.; Elghanian, R.; Mirkin, C. A.; Letsinger, R. L. *Langmuir* **2002,** 18, 6666−6670.

(2) Boland, T.; Ratner, B. D. *Langmuir* **1994**,*10*, 3845−3852.

(3) Boland, T.; Ratner, B. D. *Proc. Natl. Acad. Sci. U.S.A.* **1995**, *92* (12), 5297−5301.

(4) Tao, N. J.; DeRose, J. A.; Lindsay, S. M. *J. Phys. Chem.* **1993**, *97* (910), 919.

(5) Demers, L. M.; Ostblom, M.; Zhang, H.; Jang, N. H.; Liedberg, B.; Mirkin, C. A. *J. Am. Chem. Soc.* **2002**, *124* (38), 11248−11249.

(6) Östblom, M.; Liedberg, B.; Demers, L. M.; Mirkin, C. A. *J. Phys. Chem. B* **2005**, *109*, 15150−15160.

(7) Baroni, S.; Dal Corso, A.; de Gironcoli, S.; Giannozzi, P.; Cavazzoni, C.; Ballabio, G.; Scandolo, S.; Chiarotti, G.; Focher, P.; Pasquarello, A.; Laasonen, K.; Trave, A.; Car, R.; Marzari, N.; Kokalj, A. *PWSCF*, 3.1; Trieste, 2005.

(8) Perdew, J. P.; Wang, Y. *Phys. Rev. B* **1992**, *45*, 13244.

(9) Vanderbilt, D. *Phys. Rev. B* **1990**, *41* (11), 7892.

(10) Perdew, J. P.; Burke, K.; Ernzerhof, M. *Phys. Rev. Lett.* **1996**, *77*, 3865−3868.

(11) Troullier, N.; Martins, J. L. *Phys. Rev. B* **1991**, *43*, 1943−2006.

(12) Hutter, J.; Ballone, P.; Bernasconi, M.; Focher, P.; Fois, E.; Goedecker, S.; Parrinello, M.; Tuckerman, M. *CPMD*, 3.3; MPI für Festkîrperforschung and IBM Zurich Research Laboratory, 1999.

(13) Becke, A. *Phys. Rev. A* **1988**, *38*, 3098−3100.

(14) Lee, C.; Yang, W.; Parr, R. G. *Phys. Rev. B* **1988**, *37*, 785−789.

(15) Grönbeck, H.; Curioni, A.; Andreoni, W. *J. Am. Chem. Soc.* **2000**, *122*, 3839−3842.

(16) Frisch, M. J.; Trucks, G. W.; Schlegel, H. B.; Scuseria, G. E.; Robb, M. A.; Cheeseman, J. R.; Montgomery, J. A., Jr.; Vreven, T.; Kudin, K. N.; Burant, J. C.; Millam, J. M.; Iyengar, S. S.; Tomasi, J.; Barone, V.; Mennucci, B.; Cossi, M.; Scalmani, G.; Rega, N.; Petersson, G. A.; Nakatsuji, H.; Hada, M.; Ehara, M.; Toyota, K.; Fukuda, R.; Hasegawa, J.; Ishida, M.; Nakajima, T.; Honda, Y.; Kitao, O.; Nakai, H.; Klene, M.; Li, X.; Knox, J. E.; Hratchian, H. P.; Cross, J. B.; Bakken, V.; Adamo, C.; Jaramillo, J.; Gomperts, R.; Stratmann, R. E.; Yazyev, O.; Austin, A. J.; Cammi, R.; Pomelli, C.; Ochterski, J. W.; Ayala, P. Y.; Morokuma, K.; Voth, G. A.; Salvador, P.; Dannenberg, J. J.; Zakrzewski, V. G.; Dapprich, S.; Daniels, A. D.; Strain, M. C.; Farkas, O.; Malick, D. K.; Rabuck, A. D.; Raghavachari, K.; Foresman, J. B.; Ortiz, J. V.; Cui, Q.; Baboul, A. G.; Clifford, S.; Cioslowski, J.; Stefanov, B. B.; Liu, G.; Liashenko, A.; Piskorz, P.; Komaromi, I.; Martin, R. L.; Fox, D. J.; Keith, T.; Al-Laham, M. A.; Peng, C. Y.; Nanayakkara, A.; Challacombe, M.; Gill, P. M. W.; Johnson, B.; Chen, W.; Wong, M. W.; Gonzalez, C.; Pople, J. A. *Gaussian 03*, C.02; Gaussian, Inc: Wallingford, CT, 2004.

(17) Møller, C.; Plesset, M. S. *Phys. Rev.* **1934**, *46* (7), 618.

(18) Schwerdtfeger, P.; Dolg, M.; Schwarz, W. H. E.; Bowmaker, G. A.; Boyd, P. D. W. *J. Chem. Phys.* **1989**, *91* (3), 1762−1774.

(19) Simon, S.; Duran, M.; Dannenberg, J. J. *J. Chem. Phys.* **1996**, *105* (24), 11024−11031.

(20) Lindhal, E.; Hess, B.; van der Spoel, D. *J. Mol. Model.* **2001**, *7*, 306−317.

(21) Van Gusteren, W. F.; Billeter, S. R.; Eising, A. A.; Hunenberger, P. H.; Kruger, P. K. H. C.; Mark, A. E.; Scott, W. R.; Tironi, I. G. *Biomolecular Simulation*: *The GROMOS96 Manual and User Guide*; Hochschulverlag AG: Zürich, Switzerland, 1996.

(22) Darden, T. A.; York, D. *J. Chem. Phys.* **1993**, *98*, 10089−10094.

(23) Berendsen, H. J. C.; Postma, J. P. M.; van Gunsteren, W. F.; DiNola, A.; Haak, J. R. *J. Chem. Phys.* **1984**, *81*, 3684−3690.

(24) Lambropoulos, N. A.; Reimers, J. R. *J. Chem. Phys.* **2002**, *116* (23), 10277−10285.

(25) Bilic, A.; Reimers, J. R.; Hush, N. S.; Hafner, J. *J. Chem. Phys.* **2002**, *116* (20), 8981−8987.

(26) Kryachko, E. S.; Remacle, F. *J. Phys. Chem. B* **2005**, *109*, 22746−22757.

(27) Wetterer, S. M.; Lavrich, D. J.; Cummings, T.; Bernasek, S. L.; Scoles, G. *J. Phys. Chem. B* **1998**, *102*, 9266−9275.

(28) Bilic, A.; Reimers, J. R.; Hush, N. S. *J. Phys. Chem. B* **2002**, *106*, 6740−6747.